Smectic phases of semiflexible manifolds: Constant-pressure ensemble

Lianghui Gao and Leonardo Golubović
Physics Department, West Virginia University, Morgantown, West Virginia 26506-6315
(Received 31 January 2002; revised manuscript received 12 July 2002; published 27 November 2002)

We pursue the constant-pressure ensemble approach to elucidate the statistical mechanics of the smectic phases of semiflexible manifolds, such as two-dimensional smectic phases of long semiflexible polymers and three-dimensional lamellar fluid membrane phases. We use this approach to consider in detail sterically stabilized phases of semiflexible polymers in two-dimensional (2D) smectic systems. For these 2D systems, we obtain the universal constants characterizing the entropic repulsion between semiflexible polymers, such as those in the osmotic pressure $P=\alpha(k_BT)^{4/3}/\kappa^{1/3}(a-a_{min})^{5/3}$ with α found here to be $\cong 0.432$ (here, a is the smectic phase period, and a_{min} and κ are the polymer cross-sectional diameter and bending rigidity constant, respectively). We address, by numerical simulations and analytic arguments, finite stacks of N semiflexible manifolds, and discuss in detail the practically interesting thermodynamic limit $N\to\infty$. We show that the thermodynamic limit is quickly approached within the constant-pressure ensemble: Already from numerical simulations involving just few semiflexible polymers under constant isotropic pressure, one can obtain the infinite 2D smectic equation of state within a few percent accuracy. We use our results to discuss the competition of electrostatic and entropic effects in quasi-2D smectic phases of DNA-cationic-lipid complexes. We use our quantitative results to discuss in detail the elasticity, topological defects, anomalous elasticity, and the effects of externally applied tension in sterically stabilized 2D smectic phases of long semiflexible polymers.

DOI: 10.1103/PhysRevE.66.051918 PACS number(s): 87.15.−v, 61.30.Jf, 82.70.Kj

I. INTRODUCTION

Over recent years, we have witnessed an increased experimental and theoretical interest in structural and thermodynamic properties of two-dimensional (2D) smectic-*A* phases [1,2]. In part, it has been stimulated by the recent discovery of such a phase of long DNA molecules intercalated between lipid membranes in DNA-cationic-lipid complexes [3–8]. In these systems, long semiflexible DNA molecules themselves form stacks of one-dimensional smectic layers that are 2D analogs of lamellar fluid membrane phases and other three-dimensional smectic *A* phases [9–13]. Because of the prominent effects of thermal fluctuations in these phases, smectics and smecticlike phases continue to remain in the focus of theoretical and experimental statistical physics. At long length scales (compared to the smectic-phase period a), thermal fluctuations are responsible for the absence of true long range positional order of smectic layers [1,14,15], as well as for the anomalous elastic behavior present in both two-dimensional and three-dimensional smectics [2,16]. On the other hand, thermal fluctuations in smectics may have significant effects also on *mesoscopic* length scales. Thus, fluctuations completely dominate substantial experimental properties of sterically stabilized smectic phases of large semiflexible manifolds, such as stacks of fluid membranes (lamellar phases) or semiflexible polymers interacting with purely hard-core repulsion. In these lyotropic smectics, elastic constants and the smectic equation of state, which relates the isotropic osmotic pressure P to the smectic period a, are all purely entropic in origin [9–11,17–22]. These properties are dominated by strong fluctuations of thermally rough manifolds forming smectic stacks, as pointed out, for the first time, by Helfrich [17]. In these smectics, semiflexible manifolds are essentially free objects up to a mesoscopic length scale equal to the lateral separation between collisions of a manifold with neighboring manifolds in the stack. The confinement of manifolds by their neighbors in the stack yields a reduction of their entropy (i.e., increase in free energy) giving rise to the entropic osmotic pressure in these sterically stabilized smectics. For the case of fluid membranes, the issues related to this effect have been investigated in a number of theoretical and experimental studies on lamellar phases [9,10,17,22]. The interest in these entropic phenomena goes beyond the lamellar phases. In particular, they play a significant role in global theories of phase equilibria in fluid membrane systems [23].

In realistic smectic materials, similar entropic effects may be substantial also in the situations in which the interactions between semiflexible manifolds are not purely steric. Significant smectic properties (elastic constants, equation of state, etc.) typically result from a subtle interplay between entropic effects and bare interactions between manifolds. In this paper, we pursue the *constant-pressure ensemble* approach to address the statistical mechanics of smectic phases of flexible manifolds, such as two-dimensional smectic phases of long semiflexible polymers and three-dimensional lamellar phases of fluid membranes, with arbitrary form of the interactions between manifolds, see Sec. II. This approach is used, in the Sec. III, to consider in detail entropically stabilized 2D systems of long semiflexible polymers with hard-core repulsion. Such systems are stabilized purely by steric entropy [18–20]. For these 2D smectic stacks of N semiflexible polymers fluctuating in a plane, we calculate, in the thermodynamic limit $N\to\infty$, the universal constants characterizing the strength of the entropic repulsion between semiflexible polymers.

We address, by numerical simulations and analytic arguments, finite stacks of N semiflexible manifolds, and discuss in detail the experimentally relevant but computationally expensive thermodynamic limit $N\to\infty$. We show that this thermodynamic limit is quickly approached within the constant-

pressure ensemble: Already from the numerical simulations involving just few manifolds under constant isotropic pressure, we obtain the infinite smectic equation of state within a few percent accuracy, as documented in Sec. III and further discussed in the Sec. IV A. In Sec. IV A, we also discuss the interesting problem of hairpin turn dislocations in sterically stabilized 2D smectic phases of long semiflexible polymers [8]. In Sec. IV B, we discuss entropic effects in the situations in which the interactions between flexible manifolds are not purely steric. In that section, we discuss the systems stabilized by electrostatic repulsion of the form appropriate for the quasi-2D smectics experimentally studied in DNA-cationic-lipid complexes [4]. Our findings support the suggestion of the experimental studies that the electrostatic effects dominate over the entropic effects, at least in the experimentally accessible range of interpolymer separations in DNA-cationic-lipid complexes [4]. In Sec. IV C, we address entropically stabilized 2D smectic phases of polymers under externally applied tension (stacks of directed polymers). We use these results to further highlight the rapid convergence to the $N\to\infty$ limit in the constant-pressure ensemble approach advocated in this paper. Finally, in Sec. IV D we discuss the anomalous elasticity in 2D smectic phases of long semiflexible polymers.

This paper is organized as follows: In Sec. II, we introduce the constant-pressure ensemble description of the stacks of semiflexible manifolds. In Sec. III, we apply our approach to investigate, by Monte Carlo (MC) simulations, the sterically stabilized 2D smectics comprised of long semiflexible polymers. In Sec. IV, we discuss in more detail various 2D and quasi-2D smectic systems. In the Appendix, we analytically discuss the approach to the thermodynamic limit ($N\to\infty$) behavior essential for the discussion in Sec. III. In the Appendix, we also discuss a subtle discretization scheme used to efficiently achieve the continuum limit in our MC simulations and some other details of these simulations.

II. THERMODYNAMICS OF STACKS OF FLEXIBLE MANIFOLDS

In this section, we introduce the constant-pressure ensemble approach to discuss the thermodynamics of smectic stacks of semiflexible manifolds. Figure 1 depicts a stack of N fluctuating d-dimensional manifolds such as semiflexible polymers ($d=1$) or fluid membranes ($d=2$) fluctuating in $(d+1)$-dimensional space. In Fig. 1, $h_n(\mathbf{x})$, with $n=1,2,3,\ldots,N$, signifies the local height of the nth manifold above the d-dimensional stack base area. Figure 1 conceptualizes a smectic stack fluctuating at a fixed osmotic pressure P exerted both on lateral sides of the stack as well as on the first ($n=1$) and the last ($n=N$) manifold in the stack. In this constant-pressure ensemble, various interesting quantities are functions of the osmotic pressure P. For example, the average smectic-phase period a is

$$a(P)=\left\langle \frac{h_N(\mathbf{x})-h_1(\mathbf{x})}{N-1}\right\rangle. \tag{2.1}$$

Here, $\langle\cdots\rangle$ is the equilibrium average done with respect to the microscopic smectic Hamiltonian, of the form

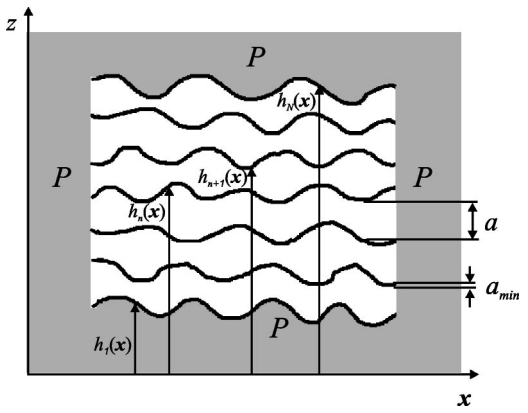

FIG. 1. Stack of N fluctuating d-dimensional flexible manifolds such as semiflexible polymers ($d=1$) and fluid membranes ($d=2$) in a $(d+1)$-dimensional space. Here, $h_n(\mathbf{x})$, with $n=1,2,3,\ldots,N$, signifies the local height of the nth manifold above the d-dimensional stack base area. The figure conceptualizes a smectic fluctuating at a fixed osmotic pressure P exerted both on lateral sides on the stack as well as on the first ($n=1$) and last ($n=N$) manifold in the stack. The average value of the smectic-phase period, i.e., the average separation between manifolds, a, is defined by the equilibrium average $a=\langle h_N(\mathbf{x})-h_1(\mathbf{x})\rangle/(N-1)$.

$$H_{sm}(h_1,\ldots,h_N)=+P\int d^d\mathbf{x}[h_N(\mathbf{x})-h_1(\mathbf{x})] + H_{com}+H_{bend}. \tag{2.2}$$

Here, the first term is the product of the *pressure and the stack volume* term, describing the coupling of the system to an externally applied *isotropic* pressure [8]. H_{com} in Eq. (2.2) is the compressional energy of the stack due to interactions between the manifolds, typically of the form

$$H_{com}=\sum_{n=1}^{N-1}\int d^d\mathbf{x}\;\; V(h_{n+1}(\mathbf{x})-h_n(\mathbf{x})). \tag{2.3}$$

$V(h_{n+1}(\mathbf{x})-h_n(\mathbf{x}))$ in Eq. (2.3) is a microscopic (bare) interaction potential between neighboring manifolds. H_{bend} in Eq. (2.2) is the bending energy of the stack due to the bending elasticity of the manifolds, of the form

$$H_{bend}=\sum_{n=1}^{N}\int d^d\mathbf{x}\frac{\kappa}{2}[\Delta h_n(\mathbf{x})]^2. \tag{2.4}$$

Here, κ is the bending (curvature) elastic constant of flexible manifolds, and $\Delta=(\partial/\partial\mathbf{x})^2$, is the d-dimensional Laplacian [21]. In thermodynamic equilibrium, the partition function, going with the smectic Hamiltonian Eq. (2.2),

$$Z=\int Dh_1\cdots\int Dh_N e^{-H_{sm}(h_1,\ldots,h_N)/k_BT}, \tag{2.5}$$

is associated with the constant-pressure free energy density defined per unit area of each manifold as

$$F(P)=-\frac{k_BT}{(N-1)A_B}\ln(Z), \tag{2.6}$$

with $A_B=\int d^dx$, the stack base area. The average smectic period, Eq. (2.1), can be obtained by differentiating the free energy density in Eq. (2.6),

$$a(P)\equiv f_d^{(N)}(P)=\left\langle \frac{h_N(\mathbf{x})-h_1(\mathbf{x})}{N-1}\right\rangle=\frac{\partial F(P)}{\partial P}. \quad (2.7)$$

The smectic equation of state can be found simply by inverting the function $f_d^{(N)}(P)$ defined in Eq. (2.7). In general, $f_d^{(N)}(P)$ can be found by solving the statistical problem involving N d-dimensional manifolds interacting through the Hamiltonian $H_{sm}(\{h_n\})$, Eq. (2.2), see Sec. III.

In the *absence* of thermal fluctuations ($T=0$), the smectic-phase period a is obtained simply by minimizing the second and the third term in Eq. (2.2), which can be more suggestively combined into a single term,

$$H'_{com}=\sum_{n=1}^{N-1}\int d^d\mathbf{x}[V(h_{n+1}(\mathbf{x})-h_n(\mathbf{x}))+P\{h_{n+1}(\mathbf{x})-h_n(\mathbf{x})\}]. \quad (2.8)$$

By minimizing Eq. (2.8) over $a=h_{n+1}-h_n$, we obtain $F(P)=[V(a)+Pa]_{\min(a)}$, yielding the "zero-temperature" (mean field) equation of state,

$$P=-\frac{\partial V(a)}{\partial a} \quad (T=0). \quad (2.9)$$

Expanding the smectic Hamiltonian Eq. (2.2) around this minimum,yields the discrete harmonic smectic elastic Hamiltonian

$$H_{el}=\int d^d\mathbf{x}\left[a\sum_{n=1}^{N}\frac{B_{sm}}{2}\left(\frac{h_{n+1}(\mathbf{x})-h_n(\mathbf{x})-a}{a}\right)^2+a\sum_{n=1}^{N}\frac{K_{sm}}{2}\left(\frac{\partial^2 h_n(\mathbf{x})}{\partial\mathbf{x}^2}\right)^2\right], \quad (2.10)$$

where

$$K_{sm}=\frac{\kappa}{a}, \quad (2.11)$$

is the smectic bending modulus and

$$B_{sm}=-a\frac{\partial P(a)}{\partial a}=a\frac{\partial^2 V(a)}{\partial a^2} \quad (T=0) \quad (2.12)$$

is the bare smectic compressibility. Introducing smectic phonon variables in Eq. (2.10), via $h_n(\mathbf{x})=u_n(\mathbf{x})+na$, and taking the continuum limit, $u_n(\mathbf{x})=u(z,\mathbf{x})$, $z=na$, yields the standard harmonic smectic elastic Hamiltonian [15]

$$H_{el}(u)=\int dz\int d^d\mathbf{x}\left[\frac{B_{sm}}{2}\left(\frac{\partial u}{\partial z}\right)^2+\frac{K_{sm}}{2}\left(\frac{\partial^2 u}{\partial\mathbf{x}^2}\right)^2\right]. \quad (2.13)$$

For *nonzero temperatures*, the pressure is given by a relation isomorphic to Eq. (2.9), with the bare interaction $V(a)$ therein replaced by a suitably defined effective interaction potential $V_{eff}(a)$. This potential is defined in the constant-volume ensemble that is related to our constant-pressure ensemble by the Legendre's transform

$$F(P)=[V_{eff}(a)+Pa]_{\min(a)}. \quad (2.14)$$

The variation over a yields

$$P=-\frac{\partial V_{eff}(a)}{\partial a}, \quad (2.15)$$

as anticipated above. With a known $F(P)$, the form of the effective potential $V_{eff}(a)$ can be obtained by inverting the Legendre transform in Eq. (2.14), by using the variational principle,

$$V_{eff}(a)=[F(P)-Pa]_{\text{ext}(P)}. \quad (2.16)$$

By extremizing here over P, we find $a=\partial F(P)/\partial P$, in accord with Eq. (2.7) above. In general (at any temperature), the smectic compressibility constant B_{sm} is defined as

$$B_{sm}=-a\frac{\partial P(a)}{\partial a}\equiv -a\left(\frac{\partial a(P)}{\partial P}\right)^{-1}, \quad (2.17)$$

where the last form is appropriate for the constant-pressure ensemble. From Eqs. (2.15), (2.7), and (2.17),

$$B_{sm}=a\frac{\partial^2 V_{eff}(a)}{\partial a^2}\equiv -a\left(\frac{\partial^2 F(P)}{\partial P^2}\right)^{-1}. \quad (2.18)$$

Notably, by comparing Eqs. (2.9) and (2.12) with Eqs. (2.15) and (2.18), we see that the entropic effects ($T\neq 0$) are incorporated by the use of the effectic potential $V_{eff}(a)$. These effects dominate the equation of state and elastic constants in the sterically stabilized smectic phases discussed hereafter in the following section.

III. ENTROPICALLY STABILIZED SMECTIC PHASES

In this section, we first discuss the equation of state of the sterically stabilized manifolds, by using our constant-pressure ensemble. Next, we apply our approach to quantitatively investigate, by MC simulations, the sterically stabilized 2D smectics comprised of long semiflexible molecules. For these two-dimensional system, we obtain here, in thermodynamic limit $N\to\infty$, the universal constant characterizing the strength of the entropic repulsion between semiflexible polymers. In sterically stabilized smectic phases, the bare interaction potential between manifolds is purely hard core,

$$V(h_{n+1}(\mathbf{x})-h_n(\mathbf{x}))=\begin{cases}0, & h_{n+1}(\mathbf{x})-h_n(\mathbf{x})>a_{min}\\ \infty, & h_{n+1}(\mathbf{x})-h_n(\mathbf{x})<a_{min}.\end{cases} \quad (3.1)$$

Here, a_{min} is the thickness of the manifolds, see Fig. 1. (For example, for semiflexible polymers in 2D smectics, a_{min} is their cross-sectional diameter.) We will first assume that

$a_{min}=0$. (Nonzero a_{min} is discussed later on in this section.) To proceed, we will use the fact that the stack model of Sec. II, Eqs. (2.2)–(2.4), has for $d<4$ (as assumed hereafter) a finite continuum limit $\Delta x\to 0$ for its correlation functions and the equation of state, see the Appendix. The $\mathbf{x}$ coordinate can be thus treated as continuous, and the model can be thus freely rescaled as

$$\mathbf{x}=Z_x\ \mathbf{x}', \quad h_n(\mathbf{x})=Z_h\ h_n'(\mathbf{x}'), \tag{3.2}$$

with arbitrary rescaling constants Z_x and Z_h. An important special feature of the hard-core potential in Eq. (3.1) is that it is *invariant* under the rescaling for $a_{min}=0$. Thus, the rescaling maps the model in Eqs. (2.2)–(2.4) into an isomorphic model with the parameters

$$P'=Z_x^d Z_h P, \quad \kappa'=Z_x^{d-4}Z_h^2\kappa, \tag{3.3}$$

whereas, from Eqs. (2.1) and (3.2), for the average period we find

$$\begin{aligned} a\left(\frac{P}{k_BT},\frac{\kappa}{k_BT}\right)&=\left\langle\frac{h_N(\mathbf{x})-h_1(\mathbf{x})}{N-1}\right\rangle_{P,\kappa,T}\\ &=Z_h\left\langle\frac{h_N'(\mathbf{x}')-h_1'(\mathbf{x}')}{N-1}\right\rangle_{P',\kappa',T}\\ &=Z_h a\left(\frac{P'}{k_BT},\frac{\kappa'}{k_BT}\right). \end{aligned} \tag{3.4}$$

The last line of Eq. (3.4) motivates to fix the rescaling constants Z_x and Z_h by the condition

$$\frac{P'}{k_BT}=\frac{\kappa'}{k_BT}=1, \tag{3.5}$$

yielding, from Eq. (3.3),

$$Z_x=\frac{(k_BT)^{1/(4+d)}\kappa^{1/(4+d)}}{P^{2/(4+d)}}, \quad Z_h=\frac{(k_BT)^{4/(4+d)}}{\kappa^{d/(4+d)}P^{(4-d)/(4+d)}}, \tag{3.6}$$

and, from Eq. (3.4),

$$a(P)=\beta_N(d)(k_BT)^{4/(4+d)}/\kappa^{d/(4+d)}P^{(4-d)/(4+d)}.$$

Here,

$$\beta_N(d)=a(1,1) \tag{3.7}$$

is a universal N-dependent constant. From Eq. (3.7), $\beta_N(d)$ is simply the average period of the stack model in Eqs. (2.2)–(2.4) with all the parameters therein set to be 1 ($P\to 1$, $k_BT\to 1$, and $\kappa\to 1$, as used in our simulations discussed later on). Thus, the smectic equation of state has the form

$$P(a)=\alpha_N(d)\frac{(k_BT)^{4/(4-d)}}{\kappa^{d/(4-d)}a^{(4+d)/(4-d)}}, \tag{3.8}$$

with

$$\alpha_N(d)=(\beta_N(d))^{(4+d)/(4-d)}. \tag{3.9}$$

We would like to stress that, with appropriate values of $\beta_N(d)$ and $\alpha_N(d)$, Eq. (3.8) applies to stacks with an *arbitrary* number N of flexible manifolds. Thus, for example, the equation of state of the finite stack, Eq. (3.8), differs from that of the infinite one only through the value of the N-dependent prefactor $\alpha_N(d)$. By the aforementioned expression for $a(P)$ and Eq. (2.7), the constant-pressure ensemble free energy density has the form

$$F(P)=\beta_N(d)\frac{4+d}{2d}\frac{(k_BT)^{4/(4+d)}P^{2d/(4+d)}}{\kappa^{d/(4+d)}}+F(P=0). \tag{3.10}$$

Further, from Eqs. (3.10) and (2.16), we obtain the effective potential in the form

$$V_{eff}(a)=\alpha_N(d)\ \frac{4-d}{2d}\ \frac{(k_BT)^{4/(4-d)}}{\kappa^{d/(4-d)}a^{2d/(4-d)}}+F(P=0). \tag{3.11}$$

In Eqs. (3.10) and (3.11), $F(P=0)$ is the free manifold ($P\to 0$) free energy. It is just a cutoff dependent constant not affecting the equation of state, B_{sm}, etc. It may be thus ignored, as done in the following. From Eqs. (3.8) and (2.17), one easily finds the associated smectic compressibility

$$B_{sm}=-a\frac{\partial P(a)}{\partial a}=\alpha_N(d)\ \frac{4+d}{4-d}\ \frac{(k_BT)^{4/(4-d)}}{\kappa^{d/(4-d)}a^{(4+d)/(4-d)}}. \tag{3.12}$$

In the above discussion, we set the thickness of the manifolds $a_{min}=0$. For a nonzero a_{min}, however, the problem can be mapped *exactly* to that with $a_{min}=0$, by making the shift

$$h_n(\mathbf{x})=\overline{h}_n(\mathbf{x})+na_{min}. \tag{3.13}$$

From Eqs. (3.13) and (3.1), it is easy to see that the new variables $\overline{h}_n(\mathbf{x})$ interact through the hard-core potential with $a_{min}=0$. So, the problem for $\{h_n(\mathbf{x})\}$ with $a_{min}\neq 0$ is mapped into the problem for $\{\overline{h}_n(\mathbf{x})\}$ with $a_{min}=0$. Consequently, from Eq. (3.13), we have, for the smectic-phase period

$$\begin{aligned} a(P)&=\left\langle\frac{h_N(\mathbf{x})-h_1(\mathbf{x})}{N-1}\right\rangle_{a_{min}\neq 0}\\ &=\left\langle\frac{\overline{h}_N(\mathbf{x})-\overline{h}_1(\mathbf{x})}{N-1}\right\rangle_{a_{min}=0}+a_{min}. \end{aligned} \tag{3.14}$$

Thus,

$$a(P)=\beta_N(d)\frac{(k_BT)^{4/(4+d)}}{\kappa^{d/(4+d)}P^{(4-d)/(4+d)}}+a_{min}. \tag{3.15}$$

TABLE I. Universal constants $\beta_N(1)$ and $\alpha_N(1)=[\beta_N(1)]^{5/3}$ for 2D stacks of N semiflexible polymers with hard-core repulsion, in the constant-pressure ensemble. The error bars are upper bounds to the actual errors induced by the ergodic averaging over a long but finite MC time. We also include the values for $\beta_\infty(1)$ and $\alpha_\infty(1)$ obtained by fitting to Eq. (3.17), see Fig. 2.

N	$\beta_N(1)$	$\alpha_N(1)$
2	0.6456 ± 0.0009	0.482 ± 0.001
3	0.6399 ± 0.0009	0.475 ± 0.001
4	0.634 ± 0.001	0.468 ± 0.001
5	0.631 ± 0.001	0.464 ± 0.001
6	0.626 ± 0.001	0.458 ± 0.002
7	0.626 ± 0.001	0.458 ± 0.002
8	0.625 ± 0.001	0.456 ± 0.002
9	0.621 ± 0.002	0.452 ± 0.002
10	0.619 ± 0.002	0.450 ± 0.002
∞	0.604[a]	0.432[a]

[a]Obtained by the extrapolation formula in Eq. (3.17).

From Eq. (3.15), the osmotic pressure $P(a)$ and the effective potential $V_{eff}(a)$ are given as in Eqs. (3.8) and (3.11), with a therein replaced by $a-a_{min}$. This confirms the usually made heuristic assumption that finite thickness effects can be incorporated by a naive replacement of a by $a-a_{min}$ [24]. We stress however that, for $a_{min}\neq 0$, the smectic compressibility, Eq. (2.17), has the form

$$B_{sm}=-a\frac{\partial P(a)}{\partial a}=\alpha_N(d)\,\frac{4+d}{4-d}\,\frac{(k_BT)^{\frac{4}{(4-d)}}\;a}{(\kappa)^{d/(4-d)}(a-a_{min})^{8/(4-d)}}. \tag{3.16}$$

From Eq. (3.16), we see that the replacement $a\to a-a_{min}$ in Eq. (3.12) would yield an *incorrect* formula for the steric smectic compressibility constant B_{sm}.

As noted below Eq. (3.7), to calculate the universal constants $\beta_N(d)$ and $\alpha_N(d)$, it suffices to study the system with $a_{min}=0$ and the parameters k_BT, κ, and P all set to be 1 (in the continuum limit $\Delta x\to 0$): For this choice of the parameters, the average stack period $a(P)$ is exactly equal to $\beta_N(d)$. If $\beta_N(d)$ is known, the corresponding value of $\alpha_N(d)$ can be directly obtained from Eq. (3.9). The average period $a(P)$ of the stacks of manifolds can be directly obtained by MC simulation of the constant-pressure ensemble Hamiltonian; see Eqs. (2.1)–(2.5). An essential part of the MC simulation is achieving the continuum limit $\Delta x\to 0$. It has been accomplished by a careful discretization scheme discussed in the Appendix. Hereafter, we focus on 2D stacks of long semiflexible polymers ($d=1$). The simulation results for $\beta_N(1)$ and $\alpha_N(1)$ for the stacks with $N=1,2,\ldots,10$ polymers are listed in Table I. The table also contains the values of $\beta_\infty(1)$ and $\alpha_\infty(1)$ for an infinite number of polymers $N\to\infty$. These two thermodynamic limit constants are obtained from the analytical treatment of the system presented in the Appendix. As discussed therein, one has the asymptotic expansion

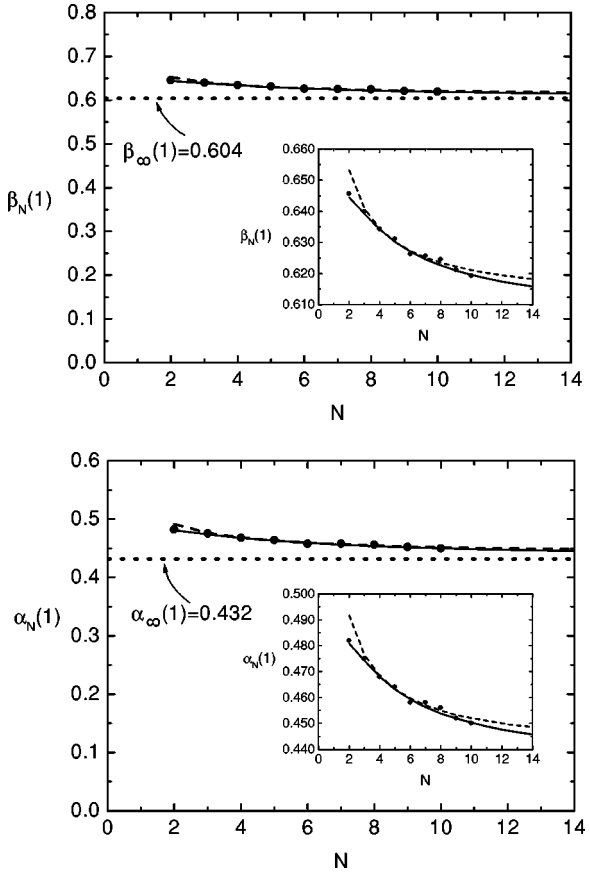

FIG. 2. Universal constant $\beta_N(1)$ and $\alpha_N(1)=[\beta_N(1)]^{5/3}$ for 2D stacks of N semiflexible polymers. Dots are the MC simulation results. Solid line is the fit to Eq. (3.17) with $\beta_\infty(1)=0.604$, $C_{(1)}=0.216$, and $C_{(3/2)}=-0.191$. In making this fit we discarded the point $N=2$. Dashed line is the fit to Eq. (3.19) with $\beta_\infty(1)=0.610$ and $C_1=0.465$. In making this fit we also discarded the point $N=2$. We note that the fitting formulas in Eqs. (3.17) and (3.19) are expected to work well for large enough N (see Sec. III and the Appendix). Still, as seen in the magnification insets, all ten simulations are well fit by both formulas. The figure documents a high efficiency of the constant-pressure ensemble in approaching the thermodynamic limit $N\to\infty$: Note that both $\beta_N(1)$ and $\alpha_N(1)$ change only by about 5% as N changes between 4 and ∞.

$$\beta_N(1)=\beta_\infty(1)+\frac{C_{(1)}}{N}+\frac{C_{(3/2)}}{N^{3/2}}+\frac{C_{(2)}}{N^2}+\frac{C_{(5/2)}}{N^{5/2}}+\cdots, \tag{3.17}$$

valid for large $N\gg 1$. By fitting the data from Table I to Eq. (3.17), one can estimate $\beta_N(1)$ as well as the universal constants in the expansion Eq. (3.17). By using this procedure, we estimate $\beta_\infty(1)\cong 0.604$, see Fig. 2. From Eq. (3.9), this corresponds to

$$\alpha_\infty(1)=[\beta_\infty(1)]^{5/3}\cong 0.432, \tag{3.18}$$

with a $\simeq 1\%$ error (upper bound), corresponding to the typical accuracy of the various data in Table I, set, as usual, by performing the ergodic average over a long but finite MC time.

In the Appendix, we also discuss an approximative closed formula for $\beta_N(1)$, of the form

$$\beta_N(1)=\beta_\infty(1)+C_1[\Psi_N(1)-\Psi_\infty(1)]. \tag{3.19}$$

Here, C_1 is a universal constant, whereas

$$\Psi_N(1)=\frac{1}{N-1}\sum_{m=1}^{N-1}\left[1-\cos\left(m\frac{\pi}{N}\right)\right]^{1/4}. \tag{3.20}$$

For $N\to\infty$, $\Psi_N(1)\to\Psi_\infty(1)\simeq 0.9071$, as discussed in the Appendix. As detailed in the Appendix, Eq. (3.19) is obtained by a reasonable but somewhat uncontrolled approximation to $\beta_N(1)$. Still, our data could be well fit to Eq. (3.19), with $\beta_\infty(1)\cong 0.610$ and $C_1\cong 0.465$, as documented in Fig. 2.

Let us summarize our MC results on sterically stabilized 2D smectic phases of long semiflexible molecules. In the practically interesting thermodynamic limit $N\to\infty$, the smectic equation of state has the form as in Eq. (3.15) with $d=1$ and $\beta_\infty(1)\cong 0.604$. Equivalently, the stack osmotic pressure P is as in Eq. (3.8) with $d=1$, a therein replaced by $a-a_{min}$, and $\alpha_\infty(1)=[\beta_\infty(1)]^{5/3}\cong 0.432$, according to our MC simulations. Finally, we emphasize the high efficiency of the constant-pressure ensemble in aproaching the thermodynamic limit $N\to\infty$ behavior. Note that, for example, both $\beta_N(1)$ and $\alpha_N(1)$ change by about only 5% as N changes between 4 and ∞, see Table I and Fig. 2. Thus, already from the numerical simulations involving a few flexible manifolds, one can obtain the infinite smectic equation of state within a few percent accuracy. In the following sections (see Secs. IV A and IV C), we discuss the physical reason beyond this favorable feature of the constant-pressure ensemble, and compare it to related earlier studies of smectic stacks.

IV. DISCUSSIONS

In the light of the results of previous sections, in this section we first continue our discussions of entropically (sterically) stabilized 2D smectics. We address in more detail their elasticity and the structural properties of topological defects (hairpin turn dislocations) in these phases in Sec. IV A. Next, in Sec. IV B, we will discuss entropic effects in the situations in which the interactions between flexible manifolds are not purely steric, by focusing on the systems stabilized by electrostatic repulsion forces of the form appropriate for the quasi-2D smectics experimentally studied in DNA-cationic-lipid complexes [4]. In Sec. IV C, we discuss entropically stabilized 2D smectic phases of semiflexible polymers under externally applied tension (stacks of directed polymers). In Sec. IV D, we discuss the anomalous elasticity phenomena in 2D smectic phases of long semiflexible polymers.

A. Sterically stabilized two-dimensional smectics

2D smectics with purely hard-core repulsion interaction between neighboring polymers are 2D analogs of extensively studied 3D lamellar phases of membranes repelling each other with a short range repulsion [17,9–11]. Like the membrane phases, in the absence of long range repulsion, interactions between long molecules are dominated by entropic effects. They yield an effective long range potential of the form as in Eq. (3.12) with $d=1$ and a therein replaced by $a-a_{min}$. In the experimentally interesting thermodynamic limit $N\to\infty$, the prefactor $(4-d)\alpha_N(d)/2d$ in Eq. (3.12) reduces to

$$A_\infty=\tfrac{3}{2}\alpha_\infty(1)\cong 0.648, \tag{4.1}$$

according to our simulations [see Eq. (3.18)]. In these systems, a_{min} is the cross-sectional diameter of polymers representing the smallest possible value of the smectic-phase period a. a_{min} is typically much smaller than semiflexible polymer persistence length $\xi_p=2\kappa/k_BT$ (e.g., for DNA molecules, $a_{min}=2$ nm, whereas $\xi_p=50$ nm [3–5]). Here, we want to emphasize that Eq. (3.11), with the universal prefactor $A_\infty=3\alpha_\infty(1)/2\cong 0.648$, is strictly appropriate only for the thermodynamic limit in which the number of polymers $N\to\infty$ (bulk behavior). It is however instructive to recall that for $N=2$ polymers, we find, within the constant-pressure ensemble, $A_2=3\alpha_2(1)/2\cong 0.723$ (see Table I). This is only 10% larger than the thermodynamic limit value A_∞ in Eq. (4.1). For comparison, for a single ($N=1$) polymer between two hard walls at the distance a, one has the free energy as in Eq. (3.11) with the prefactor $A\approx 1.1036$, as found by Burkhardt (by an exact transfer matrix calculation [20]). This is almost two times bigger than the $N=\infty$ thermodynamic limit value A_∞ in Eq. (4.1) obtained by using our constant-pressure ensemble. Notably, although A_∞ must have the same value in any ensemble, our constant pressure ensemble provides significantly faster convergence to the thermodynamic limit $N\to\infty$ behavior than the ensemble of N manifolds between hard walls. Apparently, from our Table I, we see that the thermodynamic limit result is reached, within a few percent accuracy, already by using simulations involving small stacks of just few polymers fluctuating at constant pressure P. Such a small stack, with P acting over the arc length of the last and first polymer [see Eq. (2.2) and Fig. 1], can be thought (approximately) as a subsystem of an infinite smectic stack. Within this approximation, the pressure P models the action of the infinite smectic on its small susystem, i.e., the small stack. The quick convergence to $N\to\infty$ behavior well documents this assumption. In fact, the thermodynamic limit results are reasonably approximated (within a 10% accuracy) already by using just $N=2$ polymers fluctuating under the pressure P. Apparently, this manifold-pair system well approximates a bilayer subsystem of an infinite smectic stack, with the pressure P (acting on the pair) mimicking the interaction of the bilayer with neighboring manifolds in the stack. This is in contrast to the previous related studies that have been based on considering a stack of N manifolds confined between two hard walls [20,22]. The two hard walls may be thought of as immobile *infinitely* rigid manifolds. Obviously, such a system does *not* directly resemble a subsystem of an infinite smectic. On the other side, in our constant-pressure ensemble, instead of the hard walls, we have, at the bottom and at the top, the two manifolds having the *same* bending rigidity as any other manifold in the stack.

As depicted in Fig. 1, the shapes of these boundary manifolds are thus free to fluctuate under the influence of nearby manifolds and the externally applied pressure P. This pressure applied to boundary manifolds approximately models the action of the manifolds that would be present, in an infinite smectic stack, above and below the stack in Fig. 1. Due to these physical reasons, our constant-pressure ensemble provides a faster convergence to the thermodynamic limit behavior, compared to the studies employing hard walls as boundaries (see also Sec. IV C and Ref. [28] for further discussion).

Various bulk properties of the sterically stabilized 2D smectics are sensitive to the actual value of A_∞ given by Eq. (4.1). Thus, the smectic compressibility constant is given here by Eq. (3.16) for $d=1$ [then the prefactor therein reduces to $5\alpha_\infty(1)/3=10A_\infty/9=0.720$] We note that, whereas the osmotic pressure P and the smectic compressibility B_{sm} are both sensitive to the value of A_∞, their ratio is not,

$$\Omega=\frac{P}{B_{sm}}=\frac{3}{5}\left(1-\frac{a_{min}}{a}\right). \tag{4.2}$$

Still, most of the interesting materials properties here depend on the actual value of A_∞. For example, the smectic penetration length $\lambda=(K_{sm}/B_{sm})^{1/2}$ is, from Eqs. (3.16) and (2.11),

$$\begin{aligned}\lambda&=\frac{3}{\sqrt{10A_\infty}}(\xi_p/2)^{2/3}a^{1/3}\left(1-\frac{a_{min}}{a}\right)^{4/3}\\&=1.19(\xi_p/2)^{2/3}a^{1/3}\left(1-\frac{a_{min}}{a}\right)^{4/3}.\end{aligned} \tag{4.3}$$

Many other significant structural properties of these phases also depend on the actual value of A_∞. An interesting example for this are the properties of hairpin turn dislocations recently elucidated in Ref. [8]. These dislocations have a large void in their cores, with the size along the smectic z direction $D_{eq}\gg a$, and the lateral size along the smectic x direction $L_{eq}\gg a$ [8]. From the results of Sec. V of Ref. [8], and our Eq. (4.1), we find

$$\begin{aligned}D_{eq}&=C^{4/5}\left(\frac{5}{3}\right)^{1/5}\left(\frac{3}{\sqrt{10A_\infty}}\right)^{3/5}(\xi_p/2)^{2/5}(a-a_{min})^{3/5}\\&=1.42(\xi_p/2)^{2/5}(a-a_{min})^{3/5},\end{aligned} \tag{4.4}$$

$$\begin{aligned}L_{eq}&=C^{2/5}\left(\frac{5}{3}\right)^{3/5}\left(\frac{3}{\sqrt{10A_\infty}}\right)^{4/5}(\xi_p/2)^{8/15}(a-a_{min})^{7/15}\\&=1.67(\xi_p/2)^{8/15}(a-a_{min})^{7/15},\end{aligned} \tag{4.5}$$

with $C\approx 1.198$ [8] and A_∞ as in our Eq. (4.1). Another property of these dislocation cores is the radius of the void interface curvature (induced by the osmotic pressure) R_{eq} [8]. From the results of Ref. [8] and our Eq. (4.1),

$$\begin{aligned}R_{eq}&=\frac{5}{3}\ \frac{3}{\sqrt{10A_\infty}}(\xi_p/2)^{2/3}(a-a_{min})^{1/3}\\&=1.98(\xi_p/2)^{2/3}(a\ -a_{min})^{1/3}.\end{aligned} \tag{4.6}$$

Likewise, for the hairpin dislocation energy-temperature ratio, we find

$$\begin{aligned}\frac{E_{hp}}{2k_BT}&=C^{6/5}\left(\frac{5}{3}\right)^{4/5}(\sqrt{10\ A_\infty}/3)^{3/5}\left(\frac{\xi_p/2}{a-a_{min}}\right)^{3/5}\\&=1.69\left(\frac{\xi_p/2}{a-a_{min}}\right)^{3/5}.\end{aligned} \tag{4.7}$$

We remark that the results in Eqs. (4.4)–(4.7) are applicable in the range of smectic periods a for which Eq. (4.4) yields $D_{eq}>a$. From Eq. (4.4), we find

$$\begin{aligned}\frac{D_{eq}}{a}&=C^{4/5}\left(\frac{5}{3}\right)^{1/5}\left(\frac{3}{\sqrt{10A_\infty}}\right)^{3/5}\left(\frac{\xi_p/2}{a}\right)^{2/5}\left(1-\frac{a_{min}}{a}\right)^{3/5}\\&=1.42\left(\frac{\xi_p/2}{a}\right)^{2/5}\left(1-\frac{a_{min}}{a}\right)^{3/5},\end{aligned} \tag{4.8}$$

valid in the range of a in which $D_{eq}/a>1$ [8]. From Eq. (4.8), the D_{eq}/a ratio reaches its maximum value

$$\begin{aligned}\left(\frac{D_{eq}}{a}\right)_{max}&=C^{4/5}\left(\frac{3}{25}\right)^{2/5}\left(\frac{3}{\sqrt{10\ A_\infty}}\right)^{3/5}\left(\frac{\xi_p}{a_{min}}\right)^{2/5}\\&=0.55\left(\frac{\xi_p}{a_{min}}\right)^{\frac{2}{5}},\end{aligned} \tag{4.9}$$

when the smectic period a reaches the characteristic value $a_o=\frac{5}{2}a_{min}$. By Eq. (4.9), this maximum is controlled by the ratio ξ_p/a_{min}, which is large for realistic semiflexible polymers. From Eqs. (4.8) and (4.9), the equilibrium size of hairpin turns D_{eq} is generally larger than the smectic-phase period a. The ratio $D_{eq}/a\to 1$ only in two characteristic limits: for small periods $a<a'_{min}$, with $(a'_{min}-a_{min})/a'_{min}=0.56\,(2a_{min}/\xi_p)^{2/3}$. The other limit corresponds to a highly swollen phase with the period a given by $a_{max}=(C^2/2)(5/3)^{1/2}(3/\sqrt{10\ A_\infty})^{3/2}\xi_p=1.80\xi_p$, at the border line for the phase transition to the isotropic liquid state of polymers (in analogy to the 3D fluid membrane phases [23]). Close to this transition, from Eq. (4.7) with $a\approx\xi_p$, one has $E_{hp}\approx k_BT$, and the dislocations ensemble becomes dense, in accord with the onset of a nearby isotropic liquid phase. It should be stressed though that applying results such as Eqs. (4.4)–(4.9) to a situation with $a\sim\xi_p$ yields only sound qualitative conclusions: The basic form of the entropic repulsion (3.11) is exact only in the limit $a\ll\xi_p$. As the phase period a approaches the polymer persistence length ξ_p, crumpling effects that soften the bending rigidity of semiflexible polymers come into play [11,21]. These effects are ignored here, by using the harmonic model for bending elasticity (see Sec. II). Whereas an investigation of these effects is beyond our

scope here ($a \ll \xi_p$), we note that detailed discussions of the crumpling effects in fluid membrane phases are presented in Refs. [11,23].

B. DNA-cationic-lipid complexes

A number of recent experimental studies of semiflexible polymers phases have addessed the quasi-two-dimensional smectic phases of DNA molucules with periods $a \ll \xi_p$ [3–5]. Notably, however, in these systems, the interactions between the semiflexible polymers are definitely *not* purely hard core (steric). These systems are complexes of long λ-DNA molecules mixed with cationic-lipid molecules for the purpose of modern gene therapy techniques [3]. These complexes have been the subjects of a number of recent experimental and theoretical studies [3–8]. Frequently, the complexes form a 3D lamellar membrane phase with λ-DNA molecules intercalated in galleries between lipid membranes [3,4]. Interactions between DNA molecules in different galleries are experimentally evidenced to be weak. To a good approximation, one can consider these so-called sliding phases [6,7] as stacks of weakly interacting 2D smectics in which DNA molecules play the role of smectic layers. These quasi 2D smectic phases are stabilized by complex repulsive interactions of electrostatic origin [3,4]. Their detailed form is not well known. To discuss the interplay between the entropic and electrostatic effects in these phases, we consider the following semiempirical form for the (electrostatic) osmotic pressure between DNA molecules:

$$P^{(es)}(a) = C_e \frac{k_B T}{l_B (a - a_{es})}, \quad C_e \approx 7.2 \pm 0.6, \tag{4.10}$$

suggested by Salditt *et al.*, Ref. [4]. Here, l_B is the so-called Bjerrum length; $l_B \approx 0.7$ nm in water at room temperature. a_{es} in Eq. (4.10) is an electrostatic diameter of DNA; $a_{es} \approx 0.4$ nm at most, that is, one-fifth of the actual diameter of DNA (or even smaller [4]), which is $a_{min} \approx 2$ nm. The osmotic pressure $P^{(es)}$ in Eq. (4.10) would correspond to the bare interpolymer potential of the form

$$V^{(es)}(a) = -C_e \frac{k_B T}{l_B} \ln(a - a_{es}). \tag{4.11}$$

In the absence of polymer shape fluctuations, from Eqs. (4.10) and (2.9), the smectic compressibility modulus is given here by

$$B_{sm} = C_e \frac{k_B T a}{l_B (a - a_{es})^2}. \tag{4.12}$$

The quantity Ω in Eq. (4.2) here assumes the simple form, $\Omega = P/B_{sm} = 1 - a_{es}/a$. As $a > a_{min} \approx 5 a_{es}$, Ω is ≈ 1 in practical situations. The smectic penetration length here is $\lambda(a) = (K_{sm}/B_{sm})^{1/2} = \lambda_o (1 - a_{es}/a)$, with $\lambda_o = \sqrt{\xi_p l_B / 2 C_e}$. As $a > a_{min} \approx 5 a_{es}$, to a good approximation $\lambda(a) \approx \lambda_o$ and $\Omega \approx 1$. Notably, λ here does not significantly depend on the phase period a, in marked contrast to the penetration depth in entropically stabilized phases [see Eq. (4.3)]. The above bare properties would approximate the actual (renormalized) smectic properties only for the situations in which the entropic effects due to local (mesoscopic) polymer fluctuations could be ignored. It has been suggested that this was the case, at least in the previously studied systems [4]. However, a more quantitative support for this suggestion was missing, such as the actual value of the steric coupling constant $A_\infty = 3\alpha_\infty/2$, Eq. (4.1), calculated in the present work. To discuss the competition of steric and electrostatic effects, we note that at short enough inter-DNA separations a, the steric effect must dominate: Note that, for example, the steric pressure $P^{(st)}(a)$ [see Eq. (3.8) with a therein replaced by $a - a_{min}$] diverges as $a \to a_{min}$, whereas the electrostatic pressure $P^{(es)}$ in Eq. (4.10) remains finite for $a = a_{min}$. Clearly, the steric pressure will dominate in a range of small a, for $a < a_*$, with a_* signifying a crossover length scale between the steric and electrostatic regimes. a_* can be estimated simply, from the condition $P^{(st)}(a_*) = P^{(es)}(a_*)$. By using here Eqs. (3.8) (with $d = 1$ and a replaced by $a - a_{min}$) and (4.10), one finds that

$$\frac{a_*}{a_{min}} = 1 + z_*, \tag{4.13}$$

with

$$z_* \equiv \left(\frac{\alpha_\infty(1)}{C_e} \frac{l_B}{a_{min}^{2/3} (\xi_p/2)^{1/3}} \right)^{3/5} \left(1 - \frac{a_{es}}{a_{min}} \right)^{3/5} \ll 1. \tag{4.14}$$

We thus find, for $\xi_p = 50$ nm, that $z_* \approx 0.05$. Thus, the crossover length scale a_* is only some 5% larger than the DNA diameter a_{min}. At thus small inter-DNA distances, the helixes of neighboring DNA would couple. Such a locking may tranform the 2D smectic into a 2D solid. Overall, these estimates support the conjecture of the experimental studies on DNA-cationic-lipid complexes [4], that electrostatic effects dominate over the entropic effects in the investigated range of smectic-phase periods a. It should be noted though that steric effects may become dominant *also* at *large* interpolymer separations a, at which the osmotic pressure law in Eq. (4.10), and the corresponding logarithmic form of the polymer-polymer repulsion Eq. (4.11), breaks down and becomes replaced by a faster decay law with increasing a: For *bare* osmotic pressures $P(a) \sim 1/a^\gamma$ decaying faster than the steric osmotic pressure in Eq. (3.8) [i.e., $\gamma > 5/3$ for $d = 1$], the large a behavior must be dominated by the steric pressure $P^{st}(a) \sim 1/a^{5/3}$. Whereas such a steric regime has not been reached in the previous studies in DNA-lipid complexes, its plausible existence appears to be an interesting subject for future experimental investigations of these and other related systems.

C. Stacks of *N* nonintersecting lines with tension

In this section, we compare the 2D stacks of N semiflexible tensionless polymers with bending rigidity κ with the sterically stabilized stacks of N nonintersecting lines with tension. As discussed here, in the constant-pressure en-

semble, the problem with tension is exactly solvable for $N=2$ and $N=\infty$. This provides a useful reference point for a better insight into the constant-pressure ensemble advocated in this paper. Besides, the stacks of lines with tension (''directed polymers'') are interesting in their own right. In particular, they represent the actual model for semiflexible polymer phases under external tensional force that is applied to polymers. For large enough polymer separations a, the entropic repulsion between the polymers is dominated by tensional effects rather than by bending rigidity. In 2D smectic system, the presence of the tension σ adds the term

$$H_{tens}=\sum_{n=1}^{N}\int dx\frac{\sigma}{2}\left(\frac{dh_n(x)}{dx}\right)^2 \tag{4.15}$$

to the smectic stack Hamiltonian in Eq. (2.2). In the absence of tension, for $\sigma=0$, we have the osmotic pressure law as in Eq. (3.8) with $d=1$ [for simplicity, we will set $a_{min}=0$ in this section], with the universal constants $\alpha_N(1)$ calculated in Sec. III (Table I). In particular, for the stacks with $N=2$ and $N=\infty$ polymers, we found $\alpha_2(1)\cong 0.482$ and $\alpha_\infty(1)\cong 0.432$ in the constant-pressure ensemble. In the presence of tension $\sigma\neq 0$, the long scale thermal fluctuations of flexible polymers are weakened, and, at large enough a, the pressure law as in Eq. (3.8) is replaced by a faster decaying pressure law, of the form

$$P_{st}(a)=\alpha_N^{(\sigma)}(1)\,\frac{(k_BT)^2}{\sigma a^3}. \tag{4.16}$$

Equation (4.16), with the universal constant $\alpha_N^{(\sigma)}(1)$, can be established by reasonings similar to those of Sec. III, here applied to the stack of directed polymers with $\kappa=0$ and $\sigma\neq 0$. For $\kappa\neq 0$ and $\sigma\neq 0$, there is a crossover length scale

$$a_\sigma\sim\frac{(k_BT)^2\kappa}{\sigma^3}, \tag{4.17}$$

such that for $a\ll a_\sigma$, the bending elasticity κ dominates and Eq. (3.8) applies (with $d=1$), whereas for $a\gg a_\sigma$ the tension σ dominates and Eq. (4.16) applies for $d=1$. Universal constants of the tension dominated steric pressure are actually exactly known in the ensemble of N nonintersecting directed polymers (with $\kappa=0$ and $\sigma\neq 0$) confined between two hard walls that can be mapped into the 1D gas of N free fermions confined between the two hard walls [25,22]. By using this mapping *and* the equivalence between the ensembles, which applies *only* in the thermodynamic limit $N\to\infty$, we have

$$\alpha_\infty^{(\sigma)}(1)=\frac{\pi^2}{3}\cong 3.290, \tag{4.18}$$

for *both* ensembles.

On the other side, the constant-pressure ensemble with $N=2$ polymers is also exactly solvable for $\kappa=0$ and $\sigma\neq 0$. To see this, let us consider its constant-pressure Hamiltonian

$$H_{sm}(h_1,h_2)=\int dx\left\{\frac{\sigma}{2}\left(\frac{dh_1(x)}{dx}\right)^2+\frac{\kappa}{2}\left(\frac{d^2h_1(x)}{dx^2}\right)^2+\frac{\sigma}{2}\left(\frac{dh_2(x)}{dx}\right)^2+\frac{\kappa}{2}\left(\frac{d^2h_2(x)}{dx^2}\right)^2+V_{hc}(h_2(x)-h_1(x))+P[h_2(x)-h_1(x)]\right\}, \tag{4.19}$$

corresponding to the smectic stack Hamiltonian, Eqs. (2.2)–(2.4), for $N=2$ and $\sigma=0$. To proceed, we introduce new variables defined by

$$r(x)=h_2(x)-h_1(x),\quad R(x)=\frac{h_1(x)+h_2(x)}{2}, \tag{4.20}$$

the ''relative coordinate'' and ''center of mass coordinate,'' respectively. In terms of these coordinates, $H_{sm}(h_1,h_2)$ in Eq. (4.19) seperates into a sum of two Hamiltonians,

$$H_{sm}(h_1,h_2)=H_{rel}(r)+H_{\text{c.m.}}(R), \tag{4.21}$$

with the relative Hamiltonian

$$H_{rel}(r)=\int dx\left\{\frac{\sigma}{4}\left(\frac{dr(x)}{dx}\right)^2+\frac{\kappa}{4}\left(\frac{d^2r(x)}{dx^2}\right)^2+V_{hc}(r(x))+Pr(x)\right\} \tag{4.22}$$

and the harmonic center-of-mass Hamiltonian

$$H_{\text{c.m.}}(R)=\int dx\left\{\sigma\left(\frac{dR(x)}{dx}\right)^2+\kappa\left(\frac{d^2R(x)}{dx^2}\right)^2\right\}, \tag{4.23}$$

which is trivially solvable. However, to find the equation of state, one needs to solve a nontrivial statistical mechanics problem associated with the relative Hamiltonian Eq. (4.22), to find the average

$$a=\langle h_2(x)-h_1(x)\rangle=\langle r(x)\rangle \tag{4.24}$$

as the function of the pressure P. To study the tension dominated regime [Eq. (4.16)], it suffices to set $\kappa=0$ in Eq. (4.22). Such a problem can be analytically handled by the standard transfer matrix method [26], as discussed before by Netz [8], by mapping it into a one-dimensional quantum mechanics problem [27]. For the constant-pressure free energy, Netz finds

$$F_{N=2}(P)=C_{\text{Ai}}\frac{(k_BT)^{2/3}\;P^{2/3}}{\sigma^{1/3}}+F_{N=2}(0), \tag{4.25}$$

with $C_{\text{Ai}}\cong 2.337$ being the *first* zero of the Airy function. From Eqs. (4.25) and (2.7),

$$a=\beta_N^{(\sigma)}(1)\frac{(k_BT)^{2/3}}{\sigma^{1/3}P^{1/3}}, \tag{4.26}$$

with, for $N=2$,

$$\beta_2^{(\sigma)}(1)=\tfrac{2}{3}C_{\mathrm{Ai}}\cong 1.558. \tag{4.27}$$

From Eq. (4.26), one recovers the pressure law in Eq. (4.16) with

$$\alpha_N^{(\sigma)}(1)=[\beta_N^{(\sigma)}(1)]^3, \tag{4.28}$$

and thus, for $N=2$, from Eq. (4.27),

$$\alpha_2^{(\sigma)}(1)=(\tfrac{2}{3}C_{\mathrm{Ai}})^3\cong 3.783. \tag{4.29}$$

From Eq. (4.16), Eq. (4.26) applies to any N, with the universal constants $\beta_N^{(\sigma)}(1)$ and $\alpha_N^{(\sigma)}(1)$ related as in Eq. (4.28). In particular, in the thermodynamic limit $N\to\infty$,

$$\beta_\infty^{(\sigma)}(1)=[\alpha_\infty^{(\sigma)}(1)]^{1/3}=\left(\frac{\pi^2}{3}\right)^{\frac{1}{3}}\cong 1.487, \tag{4.30}$$

using the exact result in Eq. (4.18). By comparing Eq. (4.30), for $N\to\infty$, with Eq. (4.27), for $N=2$, we see that, for a given pressure P, the average interpolymer seperation a in Eq. (4.26) is decreased by less than 5% by going from the bilayer system ($N=2$) to the bulk system ($N=\infty$) fluctuating under the constant pressure P. This illustrates high efficiency of the constant-pressure ensemble in studying the thermodynamic limit $N\to\infty$ behavior. Similar efficiency has been documented before, in Sec. III, for 2D smectics without externally applied tension (see Fig. 2 and Table I). Thus, this favorable feature appears to be generic to the constant-pressure ensemble advocated in this paper. The physical reason for this has been anticipated before, at the beginning of Sec. IV A. The stacks of N manifolds fluctuating under fixed isotropic pressure P highly resemble subsystems of an infinite smectic, with the pressure P approximately modeling the action of the infinite system on the small subsystem of N smectic layers. In general, such a subsystem can be exactly described by an *effective* subsystem Hamiltonian that may be, in principle, found by integrating out of the infinite smectic partition function the layers not belonging to the small subsystem of N smectic layers, as we detail elsewhere [28]. Here we note that this effective small stack Hamiltonian is well approximated by the constant-pressure Hamiltonian of Sec. II, as evidenced by the fast convergence to the thermodynamic limit behavior documented here for semiflexible polymers smectics (with tension) and in Sec. III (without tension). This feature of the constant-pressure ensemble is documented also by the studies of the sterically stabilized stacks of tensionless membranes ($d=2$). Thus, from Netz's simulations of $N=2$ membranes under constant pressure (Sec. III), $\beta_2(2)=[\alpha_2(2)]^{1/3}\cong 0.614$, see Ref. [8]. This is only few percent bigger than the estimate for the thermodynamic limit $N=\infty$, $\beta_\infty(2)=[\alpha_\infty(2)]^{1/3}\cong 0.596$, obtained from the simulations of Gompper and Kroll of membrane stacks confined between two hard walls [22]. [By the equivalence of ensembles in the thermodynamic $N=\infty$ limit, the same value of $\beta_\infty(2)$ would be obtained in the constant-pressure ensemble.] It is interesting to note that this $\beta_\infty(2)$ for three-dimensional membrane stacks is, curiously, nearly the same as our $\beta_\infty(1)$ for two-dimensional semiflexible polymer stacks, see Sec. III. Thus

$$\beta_\infty(2)\cong\beta_\infty(1)\cong\tfrac{3}{5}. \tag{4.31}$$

Note however that, from Eq. (3.9), the corresponding values of $\alpha_\infty(d)$ are substantially different for $d=1$ and $d=2$. It would be interesting to understand the reasons beyond the (approximative) superuniversality reasons of $\beta_N(d)$ suggested by Eq. (4.31).

D. Anomalous elasticity

2D and 3D smectics A are known to have an anomalous elastic behavior at long length scales [2,16]. It qualititavely alters the character of smectic fluctuation at scales longer than certain Ginzburg length scales ξ_{GX} and ξ_{GZ}, with, for 2D smectics [2],

$$\xi_{GX}=8\pi\frac{(K_{sm})^{3/2}}{k_BTB_{sm}},\quad \xi_{GZ}=\frac{(\xi_{GX})^2}{\lambda}, \tag{4.32}$$

$\lambda=\sqrt{K_{sm}/B_{sm}}$. For 2D smectic phases of long semiflexible molecules with bending rigidity $\kappa=k_BT\xi_p/2$, from Eqs. (2.11) and (4.32),

$$\xi_{GX}=4\pi\frac{\xi_p}{a}\lambda,\quad \xi_{GZ}=16\pi^2\left(\frac{\xi_p}{a}\right)^2\lambda. \tag{4.33}$$

For the electrostatically stabilized quasi-2d smectics in the DNA-cationic-lipid complex (see Sec. IV B), $\lambda\approx 1.6$ nm and $\xi_p\approx 50$ nm, whereas the period a is 3–5 nm. Thus, from Eq. (4.33), the anomalous length scales are large compared to the smectic-phase period ($\xi_{GZ}\sim 10^4 a$), making it hard to observe the anomalous effects in the available phase monodomains in these system. On the other side, for the sterically stabilized phases (Sec. IV A), with our quantitative result for λ in Eq. (4.3), we find, from Eq. (4.33),

$$\frac{\xi_{GX}}{a}=\frac{4\pi}{2^{2/3}}\frac{3}{\sqrt{10A_\infty}}\left(\frac{\xi_p}{a}\right)^{5/3}\left(1-\frac{a_{min}}{a}\right)^{4/3}$$
$$=9.39\left(\frac{\xi_p}{a}\right)^{5/3}\left(1-\frac{a_{min}}{a}\right)^{4/3} \tag{4.34}$$

and

$$\frac{\xi_{GZ}}{a}=\frac{16\pi^2}{2^{2/3}}\frac{3}{\sqrt{10A_\infty}}\left(\frac{\xi_p}{a}\right)^{8/3}\left(1-\frac{a_{min}}{a}\right)^{4/3}$$
$$=117.97\left(\frac{\xi_p}{a}\right)^{8/3}\left(1-\frac{a_{min}}{a}\right)^{4/3}. \tag{4.35}$$

The ratios in Eqs. (4.34) and (4.35) have an interesting dependence on a: They both reach a *maximum* at characteristic values of the smectic period a; $(\xi_{GX}/a)_{max}\sim(\xi_p/a_{min})^{5/3}$ for $a=9a_{min}/5$, whereas $(\xi_{GZ}/a)_{max}\sim(\xi_p/a_{min})^{8/3}$ for $a=3a_{min}/2$. Away from these maxima, the ratios in Eqs. (4.34) and (4.35) drop down. Thus, both ratios approach the values $O(10^2)$ for $a\sim\xi_p$, i.e., close to the transition to the

isotropic liquid phase. In this limit, however, the dislocation ensemble becomes dense (see Sec. IV A, and Ref. [8]), and the nematic charater of 2D smecticlike systems [1] would preclude the existence of the length scale range with the anomalous elastic behavior. On the other side, the ratios in Eqs. (4.34) and (4.35) can be both made small in the limit of *small* smectic periods. Note that, interestingly, both ratios actually *vanish* for $a \to a_{min}$. This phenomenon is caused by the diverging behavior of $B_{sm}(a)$ for $a \to a_{min}$, see Eq. (3.16). From Eq. (4.35), for example, the ratio $\xi_{GZ}/a \to 1$ for $a \to (1+\sigma)a_{min}$, with

$$\sigma \approx \left(\frac{2^{2/3}}{16\pi^2} \frac{\sqrt{10 A_\infty}}{3} \right)^{3/4} \left(\frac{a_{min}}{\xi_p} \right)^2 = 0.028 \left(\frac{a_{min}}{\xi_p} \right)^2 \tag{4.36}$$

for the realistic semiflexible molecules, with $a_{min} \ll \xi_p$. For the DNA molecules, for example, with $\xi_p \approx 50 a_{min}$, from Eq. (4.36), $\sigma \sim 10^{-5}$. That is, $\xi_{GZ}/a \to 1$ only for a very small separation between DNA helixes. Again, as noted in the discussion below Eq. (4.14), such separations are almost certainly inaccessible within the range of the smectic phase of DNA molecules. Within the smectic range, one must require that $a - a_{min}$ is some 10% or so larger than a_{min}, to avoid crystalization into a 2D solid of locked DNA helixes. Still, even with $a \approx 1.1 a_{min}$, the ratios in Eqs. (4.34) and (4.35) would remain large for $\xi_p/a \approx \xi_p/a_{min} = 25$, as for DNA. Overall, an experimental observation of the anomalous elasticity effects may be hard to achieve in both sterically and, as noted before, electrostatically stabilized phases of long semiflexible molecules, such as DNA. The above large estimates for ξ_{GZ}/a, for example, show that one must have at disposal large monodomains of aligned DNA molecules, which may be hard to realize in the experiments [3–5].

ACKNOWLEDGMENTS

We thank Tim Salditt, Joachim Raedler, and Cyrus Safinya for discussions on various experimental aspects of DNA-cationic-lipid complexes. L. G. acknowledges support through Grant No. A/02/15054 of the Deutscher Akademischer Austauschdienst (DAAD).

APPENDIX

In this appendix, we will first analytically discuss the approach to the thermodynamic limit behavior, $N \to \infty$. We derive here the formulas used in Sec. III to extract this behavior from the simulations done with a finite number N of flexible polymers (see the end of Sec. III). We will discuss the N dependence of the average smectic-phase period Eq. (2.1). For this purpose, we consider here interpolymer potentials $V(r)$ $(r = h_{n+1} - h_n)$ such that $V_{net}(r) = V(r) + Pr$ has an analytic minimum at $r = r_0$, see Eq. (2.8) [we discuss, later on, the situations with $V_{net}(r)$ having a nonanalytic minimum]. Expanding V_{net} in powers of $r - r_0$ yields, from Eq. (2.8),

$$H'_{com} = \sum_{n=1}^{N-1} \int d^d\mathbf{x} \sum_{k=2}^{\infty} \frac{b_k}{k!} [h_{n+1}(\mathbf{x}) - h_n(\mathbf{x}) - r_0]^k, \tag{A1}$$

with $b_k = V^{(k)}(r_0)$. Introducing here the smectic phonon variables, via $h_n(\mathbf{x}) = n r_0 + u_n(\mathbf{x})$, reduces the original stack Hamiltonian (2.2) to

$$H_{sm} = H_0 + H_{anh} \tag{A2}$$

with

$$H_0 = \int d^d\mathbf{x} \left[\sum_{n=1}^{N} \frac{\kappa}{2} [\triangle u_n(\mathbf{x})]^2 + \sum_{n=1}^{N-1} \frac{b_2}{2} [u_{n+1}(\mathbf{x}) - u_n(\mathbf{x})]^2 \right], \tag{A3}$$

the harmonic part of the smectic Hamiltonian, and

$$H_{anh} = \sum_{n=1}^{N-1} \int d^d\mathbf{x} \sum_{k=3}^{\infty} \frac{b_k}{k!} [u_{n+1}(\mathbf{x}) - u_n(\mathbf{x})]^k, \tag{A4}$$

the anharmonic part of the Hamiltonian. For the average smectic period Eq. (2.1), we have

$$a_N = \left\langle \frac{h_N - h_1}{N-1} \right\rangle = r_0 + \left\langle \frac{u_N - u_1}{N-1} \right\rangle. \tag{A5}$$

In the absence of the anharmonic terms, Eq. (A4), the second term in Eq. (A5) vanishes. Thus, within the harmonic approximation, $a = r_0$, i.e., a is N independent. The N dependence of a is thus an effect of the anharmonic terms in Eq. (A4). They can be handled systematically, first by carefully diagonalizing the harmonic smectic Hamiltonain Eq. (A3), and then using the standard perturbation theory, the loop expansion [29]. For $d < 4$, this perturbation theory, to all orders, has a finite continuum limit $\Lambda_q \sim 1/\Delta x \to \infty$; see, e.g., Eq. (A6) below (see also the discussion in Ref. [26]). We assume this limit in Eqs. (A7)–(A12) hereafter. Thus, for example, by keeping in Eq. (A4) only the cubic term $(k = 3)$, we find, to one loop order (''tadpole'' diagram)

$$a_N = r_0 - \frac{N}{N-1} \frac{b_3 k_B T}{2 b_2} \int \frac{d^d q}{(2\pi)^d} \frac{1}{N} \times \sum_{m=1}^{N-1} \frac{2\left[1 - \cos\left(m \frac{\pi}{N}\right)\right]}{\kappa q^4 + 2 b_2 \left[1 - \cos\left(m \frac{\pi}{N}\right)\right]}, \tag{A6}$$

for the stack of N d-dimensional manifolds. Integrating Eq. (A6) over q yields, for $d < 4$,

$$a_N = r_0 + A_d \Psi_N(d). \tag{A7}$$

Here, A_d is an N-independent quantity $(A_d \sim -b_3)$, whereas

$$\Psi_N(d)=\frac{1}{N-1}\sum_{m=1}^{N-1}\left[1-\cos\left(m\frac{\pi}{N}\right)\right]^{d/4} \tag{A8}$$

is a dimensionless quantity responsible for the N dependence of the average smectic period in Eq. (A7). It has a finite limit for $N\to\infty$,

$$\Psi_\infty(d)=\int_0^\pi \frac{dQ}{\pi}[1-\cos(Q)]^{d/4}. \tag{A9}$$

Equation (A7) can be then, more suggestively, rewritten as

$$a_N=a_\infty+A_d[\Psi_N(d)-\Psi_\infty(d)], \tag{A10}$$

making it manifest that $a_N\to a_\infty$ as $N\to\infty$. For example, for 2D stacks of semiflexible polymers ($d=1$), $\Psi_\infty(1)=2^{1/4}B(1/2,3/4)/\pi\cong 0.9071$, whereas, from Eq. (A8), $\Psi_2(d)=1$ (for any d). These numbers exemplify the fact that, for $A_d\sim -b_3>0$, the average smectic period a_N in Eq. (A10) decreases with increasing N, [30]. This is in accord with the data in Table I, by recalling that the constant $\beta_N(1)$ therein is identical to a_N for $P=\kappa=k_BT=1$ (see Sec. III). Thus, from Eq. (A10),

$$\beta_N(d)=\beta_\infty(d)+C_d[\Psi_N(d)-\Psi_\infty(d)] \tag{A11}$$

for the sterically stabilized phases. Here, C_d is, like $\beta_N(d)$, a universal constant. As documented in Sec. III (see Fig. 2), for the case $d=1$, Eq. (A11) provides a good fit to our data obtained with different values of N. In relation to Eq. (A11), few remarks are in order.

(i) Equation (A11) is valid, to one-loop order, only for the model (A2) truncted to the cubic order. Even though Eq. (A11) provides a good fit to the data of Sec. III (see Fig. 2), it is only an approximation. The full model contains quartic, quintic, etc. anharmonicities [see Eq. (A4)]. Also, in the full treatment, one would need to do the loop expansion to all orders (a difficult, if not impossible, task). Still, an inspection of the perturbation expansion shows that, for $d=1$,

$$\beta_N(1)=\beta_\infty(a)+\frac{C_{(1)}}{N}+\frac{C_{(3/2)}}{N^{3/2}}+\frac{C_{(2)}}{N^2}+\frac{C_{(5/2)}}{N^{5/2}}+\cdots, \tag{A12}$$

as can be inferred (also) by asymptotically evaluating the sum in Eq. (A8) for $d=1$ and $N\gg 1$. Note that, for $d=1$, the expansion contains both integer and half-integer powers of $1/N$.

(ii) The reasoning leading to Eq. (A7) assumes that one deals with $V_{net}(r)=V(r)+Pr$ having an analytic minimum. Apparently, this is not the case if $V(r)$ is the hard-core potential $V_{hc}(r)$, i.e., in the sterically stabilized phases (Sec. III). Nonetheless, it is to be generally expected that the *large* N behavior in these system can be handled by a suitable *coarse-grained* effective potential having an analytic form similar to that of the effective potential discussed in Sec. III, see Eqs. (3.11) [31]. The above reasoning can be then applied to such a coarse-grained model, yielding again the expansion in Eq. (A12). Like β_N, the numerical constants in this expansion must be universal. Overall, for large enough values of N, the expansion (A12) should be applicable also to the sterically stabilized 2D stack of semiflexible polymers, as documented in Sec. III, see Fig. 2.

We now turn to the discussion of the discretization scheme used in our Monte Carlo simulation by focusing on the most subtle part related to the semiflexible polymer bending energy. In the continuum model, it has the familiar form

$$H_{bend}=\frac{\kappa}{2}\int dx h(x)\left(\frac{\partial^2}{\partial x^2}\right)^2 h(x)=\frac{\kappa}{2}\int\frac{dq}{2\pi}q^4|\tilde{h}(q)|^2 \tag{A13}$$

for each of the polymers in the stack. The straightforward discretization procedure (which is actually *not* used in the calculations presented in this paper) is to replace Eq. (A13) with

$$H_{bend}^{disc}=\frac{\kappa}{2(\Delta x)^3}\sum_k h_k(\Delta_l)^2 h_k. \tag{A14}$$

Here, as usual, $h_k=h(x)|_{x=k\Delta x}$ and Δx is the size of the polymer "unit cell" (physically, the monomer size). Δ_l in Eq. (A14) stands for the ordinary lattice Laplacian: $\Delta_l h_k=h_{k+1}-2h_k+h_{k-1}$, and, thus,

$$(\Delta_l)^2 h_k=h_{k-2}-4h_{k-1}+6h_k-4h_{k+1}+h_{k+2}. \tag{A15}$$

This simple discretization scheme can be shown to produce an "error" in equilibrium averages (relative to the continuum model, $\Delta x=0$) that is proportional to $(\Delta x)^2$. This can be seen by calculating momentum integrals such as those in Eq. (A6), with the q^4 therein replaced by its lattice version implied by Eq. (A14), yielding

$$q^4\to(q_l^2)^2=\left[\frac{2[1-\cos(q\Delta x)]}{(\Delta x)^2}\right]^2, \tag{A16}$$

with $|q|<\pi/\Delta x$, the momentum cutoff. The actual cause of the $(\Delta x)^2$ error is *not* due to the presence of this cutoff. Rather, the error of this magnitude emerges due to the fact that the right hand side of Eq. (A16) is not exactly q^4. By expanding it, one finds

$$(q_l^2)^2=q^4+\text{const}\ q^6(\Delta x)^2+\cdots, \tag{A17}$$

eventually triggering the $(\Delta x)^2$ error. Fortunately, it is possible to further diminish the error magnitude below $(\Delta x)^2$. For this purpose, in our simulation, we replace the $(\Delta_l)^2$ operator in Eq. (A14) with the lattice operator defined by

$$(\Delta_l)^2-\tfrac{1}{6}(\Delta_l)^3. \tag{A18}$$

The marked feature of the new operator in Eq. (A18) is that it yields, in the momentum representation [$\Delta_l\to -q_l^2=-2[1-\cos(\Delta x q)]/(\Delta x)^2$], the expansion

$$(q_l^2)^2+\frac{1}{6}(q_l^2)^3=q^4+0\times q^6-\frac{7}{2\times 5!}q^8(\Delta x)^4+\cdots, \tag{A19}$$

with a *vanishing* q^6 term. From Eq. (A19), one may naively expect that the discretization error is now $\sim(\Delta x)^4$. This, however, turns out to be wrong, as can be checked by calculating the momentum integrals such as those in Eq. (A6), with $(q^2)^2$ therein replaced by $(q_l^2)^2+(q_l^2)^3/6$, [with $q_l^2=2[1-\cos(q\Delta x)]/(\Delta x)^2$, as noted above]. This calculation shows that the actual error is $\sim(\Delta x)^3$ rather than $(\Delta x)^4$. Still, with the more sophisticated discretization scheme in Eq. (A18), one may get a considerable improvement over the simple scheme in Eq. (A14). In fact, in our MC calculations (Sec. III), with $\kappa\sim 1$, by employing the operator in Eq. (A18), the relative discretization error could have been made smaller than 0.5% by using $\Delta x=1/3$. We checked this error level by estimating it analytically along the lines briefly outlined above. Additionally, we checked this error by running test simulations with a smaller $\Delta x=1/6$. Throughout the simulations, the discretization error level was kept smaller than the standard MC statistical error (due to averaging over a finite MC time), which has 1% level (upper bound) for the simulations in Sec. III.

Finally, we comment on the statistical error of our MC simulations (see the Table I). As usual, the equilibrium average smectic period Eq. (2.1) is obtained from the time (ergodic) averages of the ''instantaneous'' smectic periods that are calculated at each MC cycle (1 MC cycle corresponds to sequential trial updates of all degrees of freedom once, and represents the natural time unit for MC dynamics). To estimate the statistical error for a MC simulation with t_{max} cycles, the time average of the smectic period is calculated seperately for ten time subintervals, each with $t_{max}/10$ cycles. The root-mean-square variance of these ten averages, from different subintervals, represents the statistical error of a MC simulation done over a *single subinterval* with $t_{max}/10$ cycles. These errors of subinterval averages are the errors reported in the Table I. Thus, the factual statistical error for the *entire* simulation with t_{max} MC cycles is actually *smaller* by the factor $\sqrt{10}$ than that reported in Table I. An essential condition here is that there are no substantial autocorrelations between different time subintervals. In other words, the autocorrelation function of the instantaneous smectic periods must have its time range smaller than $t_{max}/10$ cycles. The autocorrelation time range corresponds to the longest time scale in the system. It is, in fact, the lifetime of the *slowest* mode of the system. This time scale generally increases with increasing number of manifolds N, because smectics are massless systems, without intrinsic long space-time scales. At this point, it is useful to recall that the Monte Carlo dynamics is in fact qualitatively the same as the Langevin dynamics (Type *A* model, see Ref. [29]). This relation can be used to estimate the longest mode lifetime for a system with any number of manifolds N. For the smectic Hamiltonian in Eq. (A3), we thus find an interesting relation for this longest mode lifetime,

$$\tau(N)=\frac{\tau(2)}{1-\cos\left(\frac{\pi}{N}\right)}, \tag{A20}$$

for the system with N manifolds. Equation (A20) relates the longest mode lifetime for the system with N manifolds to that with twp manifolds, $\tau(2)$, which is about 500 cycles, as obtained by calculating the autocorrelation function from our MC data for $N=2$. Thus, by Eq. (A20), for our largest simulation with $N=10$ manifolds, $\tau(10)$ is about 10 000 MC cycles. With $t_{max}=3\times 10^6$ cycles, as used in our simulation, this value of $\tau(10)$ is substantially shorter than the size of the aforementioned time subintervals, $t_{max}/10=3\times 10^5$. The statistical error of the average smectic period can be shown (by using the aforementioned relationship the Langevin dynamics) to be proportional to $\sqrt{N/t_{max}L^d}$ for $t_{max}\gg\tau(N)$ (L is the lateral smectic size, here, the length of each semiflexible polymer). For uniformity, we used the same $t_{max}=3\times 10^6$ and $L=5000\Delta x$ for all simulated systems with different N. Thus, as is also evident from the Table I, the statistical errors increase with increasing N. Still, even for the largest $N=10$, this error is within 1% (see the $N=10$ line of Table I, and recall that the factual error is smaller than the error reported therein by the factor $\sqrt{10}$, as noted above).

[1] J. Toner and D.R. Nelson, Phys. Rev. B **23**, 316 (1981).

[2] L. Golubović and Z.-G. Wang, Phys. Rev. Lett. **69**, 2535 (1992); Phys. Rev. E **49**, 2567 (1994). The anomalous smectic elasticity effects, discussed in those works in 2D smectics, are actually supressed in the smectic stack model of Sec. II, by the use of vertical distances $[=h_{n+1}(\mathbf{x})-h_{n+1}(\mathbf{x})]$ in the inter-manifold interaction potentials in Eq. (2.3). Whereas this approximation still yields the standard Landau-Peierls harmonic smectic Hamiltonian (2.13), the anharmonic terms causing the anomalous elasticity are actually discarded by the artificial symmetry breaking caused by the use of vertical distances. In the present paper, we leave beyond our scope the full smectic model that includes also the anharmonicities causing the anomalous elasticity. This is, in part, because the anomalous effects are estimated to be weak in the currently studied experimental system, as discussed in Sec. IV D (see also Refs. [7,8]).

[3] J.O. Radler, I. Koltover, T. Saldit, and C.R. Safinya, Science **275**, 810 (1997).

[4] T. Salditt, I. Koltover, J.O. Radler, and C.R. Safinya, Phys. Rev. Lett. **79**, 2582 (1997); Phys. Rev. E **58**, 889 (1998).

[5] F. Artzner, R. Zantl, G. Rapp, and J.O. Radler, Phys. Rev. Lett. **81**, 5015 (1998); R. Zantl, F. Artzner, G. Rapp, and J.O. Radler, Europhys. Lett. **45**, 90 (1990).

[6] L. Golubović and M. Golubović, Phys. Rev. Lett. **80**, 4341 (1998); **81**, 5704(E) (1998); C.S. O'Hern, and T.C. Lubensky, *ibid.*, **81**, 4345 (1998).

[7] L. Golubović, T.C. Lubensky, and C.S. O'Hern, Phys. Rev. E **62**, 1069 (2000).

[8] L. Golubović, Phys. Rev. E **64**, 061901 (2001) discusses hairpin turn dislocations in 2D smectics by employing a coarse-grained, effective Hamiltonian in the constant-pressure ensemble. This is in contrast to the discussion here, focused on

the microscopic (bare) constant-pressure Hamiltonian Eq. (2.2), somewhat rarely used in the literature. See S. Leibler and R. Lipowsky, Phys. Rev. B **35**, 7004 (1987); R.R. Netz, Phys. Rev. E **51**, 2286 (1995) discusses small stacks of $N=2$ manifolds in the constant-pressure ensemble. See, also, R.R. Netz and R. Lipowski, Europhys. Lett. **29**, 345 (1995), suggesting that the thermodynamic limit $N\to\infty$ is reached already by considering $N=2$ membranes (at least within 1% accuracy). We note that our findings here clearly show that this is definitely not the case for semiflexible polymers (there is a 10% difference between the $N=2$ and $N=\infty$ results). We would like to stress that the constant-pressure ensemble is exactly related (via the Legendre tramsforms discussed in Sec. II) to the constant-volume ensemble, in the thermodynamic limit of large lateral size of manifolds (for *any* number of manifolds N, finite or infinite). From the constant-volume ensemble, here we understood the stack of manifolds with a fixed volume of space enclosed between the bottom and the top boundary manifold in Fig. 1. This ensemble should not be confused with yet another ensemble, of N manifolds fluctuating between two hard walls (see, e.g., Ref. [22]). For a *finite* N, such an ensemble is *not* related in any simple way to the constant-pressure (or constant-volume) ensemble. In particular, for the sterically stabilized systems, the constants $\alpha_N(d)$ in the expression for the osmotic pressure (see Sec. III) are different in these two ensembles (see Secs. IV A and IV C).

[9] F.C. Larche, J. Appell, G. Porte, P. Bassereau, and J. Marignan, Phys. Rev. Lett. **56**, 1700 (1986).

[10] C.R. Safinya, D. Roux, G.S. Smith, S.K. Sinha, P. Dimon, N.A. Clark, and A.M. Bellocq, Phys. Rev. Lett. **57**, 2718 (1986); see also D. Roux and C.R. Safinya, J. Phys. (Paris) **49**, 307 (1988).

[11] L. Golubović and T.C. Lubensky, Phys. Rev. B **39**, 12 110 (1989).

[12] N. Lei, C.R. Safinya, and R.F. Bruinsma, J. Phys. II **5**, 1155 (1995).

[13] R. Holyst, Phys. Rev. A **42**, 7511 (1990); R. Holyst, D.J. Tweet, and L.B. Sorensen, Phys. Rev. Lett. **65**, 2153 (1990).

[14] L.D. Landau and E. M. Lifshitz, *Statistical Physics* (Pergamon, Oxford, 1969).

[15] P.G. de Gennes and J. Prost, *Physics of Liquid Crystals* (Oxford University Press, Oxford, 1993).

[16] G. Grinstein and R.A. Pelcovits, Phys. Rev. Lett. **47**, 856 (1981); Phys. Rev. A **26**, 915 (1982).

[17] W. Helfrich, Z. Naturforsch. A **33**, 305 (1978); W. Helfrich and R.M. Servus, Nuovo Cimento D **3**, 137 (1984).

[18] T. Odijk, Macromolecules **19**, 2313 (1986); D. Roux and C. Coulon, J. Phys. (France) **47**, 1257 (1986).

[19] M. Dijkstra, D. Frenkel, and H.N.W. Lekkerkerker, Physica A **193**, 374 (1993).

[20] T.W. Burkhardt, J. Phys. A **30**, L167 (1997).

[21] For a review, see *Statistical Mechanics of Membranes and Surfaces*, edited by D.R. Nelson, T. Piran, and S. Weinberg (World Scientific, Singapore, 1989).

[22] G. Gompper and D.M. Kroll, Europhys. Lett. **9**, 59 (1989); For a review, see, D. Sornette and N. Ostrowsky, in *Micelles, Membranes, Microemulsions, and Membranes*, edited by W. M. Gelbart, A. Ben-Shaul, and D. Roux (Springer-Verlag, New York, 1994) p. 251.

[23] L. Golubović and T.C. Lubensky, Phys. Rev. A **41**, 4343 (1990); L. Golubović, Phys. Rev. E **50**, R2419 (1994); D.C. Morse, *ibid.* **50**, R2423 (1994).

[24] D. Sornette and N. Ostrowsky, J. Phys. (France) **45**, 265 (1984)

[25] V.L. Pokrovsky and A.L. Talapov, Zh, Éksp. Teor. Fiz. **78**, 269 (1980) [Sov. Phys. JETP **51**, 134 (1980)]. See also Ref. [22].

[26] See, e.g., J.B. Kogut, Rev. Mod. Phys. **51**, 659 (1979) for a discussion of the standard transfer matrix method. We remark that a generalization of the transfer matrix calculation of Netz (Ref. [8]) to the case of directed polymers with nonzero bending rigidity, $\kappa\neq 0$, is, in principle, possible but mathematically tantalizing due to considerable mathematical complexity of these analytic transfer matrix calculations (see Ref. [20], for example). Still, at least, the very existence of the transfer matrix formulation for $\kappa\neq 0$ is significant in its own right, as it provides a rigorous proof of the existence of the continuum limit $\Delta x\to 0$ for the 2D smectic stacks of semiflexible polymers $(d=1)$.

[27] L.D. Landau and E.M. Lifshitz, *Quantum Mechanics: Non-Relativistic Theory* (Pergamon, London, 1959).

[28] L. Gao and L. Golubović, (unpublished).

[29] S.-K. Ma, *Modern Theory of Critical Phenomena* (Benjamin, Reading, MA, 1976).

[30] As $A_d\sim -b_3=-V^{(3)}(r_0)$, a positive A_d corresponds to a *negative* third derivative of $V_{net}(r)=V(r)+Pr$ at r_0, i. e., a negative cubic anharmonicity constant. We note that the second term in Eq. (A6) is the similar to the familiar thermal bond expansion terms in ordinary crystals, which expand upon temperature increase if $V^{(3)}<0$. One should stress though that, in contrast to ordinary crystals, in lyotropic smectics $V(r)$ is typically purely repulsive, with no minimum. Still, $V_{net}(r)$ has such a minimum at $r=r_0\to\infty$ as $P\to 0$. Note that $A_d\sim -V^{(3)}(r_0)>0$, for example, for all repulsive potentials $V(r)$ that decay as power laws for r.

[31] Note that the third derivative of this coarse-grained potential $V_{cg}(r)$ must be negative, see the discusion above Eq. (A11). This is consistent with $V_{cg}(r)$ decaying as a power law (see Ref. [30]), much like the effective potential $V_{eff}(r)$ does in Eq. (3.12).